Proceedings of ICES2006
ASME Internal Combustion Engine Division 2006 Spring Technical Conference
May 8-10, 2006, Aachen, Germany

ICES2006-1336

NUMERICAL ANALYSIS OF A SMALL TURBO-CHARGED SPARK-IGNITION ENGINE

Gustavo Fontana, Enzo Galloni, Roberto Palmaccio
Department of Industrial Engineering, University of Cassino, Italy

Enrico Torella
ELASIS S.C.p.A. Italy

ABSTRACT

The reduction of green-house gas emissions, that is the reduction of engine fuel consumption, is becoming a primary requirement for the automotive industry as well as meeting current and future emission legislations.

Performing high torque values with small displacement engines, the so-called "downsizing", permits, in general, to limit some typical engine losses (for instance: pumping and friction losses), increasing the overall engine efficiency. This means to improve vehicle fuel economy and, as a consequence, the CO_2 emissions avoiding a performance decrease.

In this paper, the behavior of a small displacement turbo-charged spark-ignition engine prototype, for medium size passenger cars, has been analyzed.

3-D numerical simulations have been carried out in order to achieve a lot of information on engine performance and control parameters. Thus, at different engine operating points, intake and exhaust manifold pressure, volumetric efficiency, high pressure curves, the flow field of the fresh charge within the cylinder, the air to fuel ratio distribution, the residual gas fraction distribution and so long have been calculated.

Since, as usual, the turbocharged version of the engine under study derives from an existing naturally aspirated engine, the purpose of this investigation is to obtain a detailed picture of the variations produced by turbo-charging on engine main parameters. The increase of knock risk due to higher cylinder pressures has been evaluated as well.

Thanks to the three dimensional analysis, sound information have been obtained, so that suggestions for modifying some geometric engine parameters, according to the variations imposed by turbo-charging, have been proposed.

Computations have been performed by means of the 3-D AVL Fire code. Initial and boundary conditions have been evaluated by means of 1-D, unsteady computations running separately from the 3-D code.

The model utilized in this study has been validated by comparing the obtained results to the measured data provided by the research center of the engine manufacturer.

INTRODUCTION

In the last fifteen years, in Europe, great steps forward on the way of containing the emission levels from road transportation vehicles have been made. The EURO 4 emission standard has imposed very low levels for the so called regulated emissions produced by both spark-ignition and compression ignition engines.

The recent signature of Kyoto protocol has shifted the attention to the amounts of the greenhouse gas CO_2 released in the atmosphere by the internal combustion engines. The European car manufacturers reached an agreement for about 20% reduction of the fleet CO_2 levels in a few years. This target represents a demanding challenge for present spark-ignition engines. [1, 2, 3, 4, 5, 6, 7, 8].

To improve engine fuel economy, at a given power output, means to increase the energy conversion efficiency. It is known that the spark-ignition engine efficiency is variable in the engine operating map, in particular, efficiency dramatically falls with load due to the additional losses introduced by the throttle valve during the intake stroke.

Since a road engine is very frequently run under low load and low speed conditions, the improvement of the fuel consumption in these operating points leads to a significant improvement of fuel economy hence to a significant reduction of the amount of CO_2 produced.

Low swept volume engines must run at higher loads, so pumping losses are reduced by the de-throttling effect.

Performing high torque values with small displacement engines, the so-called "downsizing", permits, in general, to limit some typical engine losses and to improve fuel economy. Turbocharging, due to the increase of mean effective pressure, allows increasing the output power of small displacement engines up to the levels of larger naturally aspirated engines.

However, high cylinder pressure, high load and low engine speed, in spark-ignition engines, constitute a parameter set which considerably increases knock risk. For this reason it is necessary to think to numerous interventions at the same time (as an example: Gasoline Direct Injection, Variable Valve Actuation, Cold EGR, Variable Compression Ratio, etc.). These measures, all together well harmonized, allow obtaining the turbocharging advantages without penalizing the engine thermal efficiency as it typically happens when the volumetric compression ratio of supercharged engines is reduced.

With reference to this, Lake et al. [8] analyzed five different strategies for knock control in a turbocharged engine and, by means of several experimental tests, they highlighted the benefits coming mainly from charge dilution at high engine load. Petitjean et al. [9] have analyzed the world scenario of hundred production vehicles. Comparing naturally aspirated and turbocharged engines, at a given performance level, they have shown the advantage of engine downsizing in terms of fuel economy. Furthermore, in [10], the improved fuel economy of a downsized engine vehicle is seen in association to some advantages deriving from an electric booster supercharging system. In [11], a numerical model able to simulate the transient operation of a small turbocharged engine has been presented and the knock risk has been accounted for by the optimization of compression ratio and boost pressure.

For performance evaluation of a complicate energy system such as the internal combustion engine, Computational Fluid Dynamics (CFD) is today a well proven tool in investigating the complex phenomena taking place within the engines and it allows predicting most of the obtainable performances reducing expensive and time consuming experiments necessary in the development process of new engines or new engine parts. With reference to this, the more and more stringent requirements of reducing both fuel consumption and pollutant emissions put in evidence the utility of reliable computational models able to accurately describe the engine behavior [12, 13, 14, 15].

In this paper, the major attention has been paid to the combustion development and the problem of knock onset rather than to the estimation of engine performance. In order to analyze such aspects as combustion rate and flame front propagation, the flow field within the cylinder has been investigated. The 3-D AVL Fire code has been utilized.

THE ENGINE

The object of the research activity is a small displacement (1.368 dm^3) spark-ignition engine prototype, featuring 4 valves per cylinder, for medium size passenger cars. The target is obtaining a significantly high specific power engine with low swept volume. The solution chosen to meet this target is turbocharging.

The prototype features a "roof" type head ceiling, while the pistons are carved with an axial-symmetric bowl (Figure 1). The compression ratio is 9.8:1. Inlet port and valves, together with the combustion chamber shape generate, during both the intake phase and the following compression phase, a tumble motion, which contributes to the turbulence level.

The compressor pressure ratio is about 1.85, while inter-cooling is used to reduce the temperature of the air entering the cylinders.

Both rich mixtures and retarded ignition timing are used for knock control. These measures reduce the in-cylinder peak temperature retarding the spontaneous ignition of unburned gas.

In Figure 2, the measured torque and the measured brake specific fuel consumption at wide open throttle, at the knock limited operation are reported.

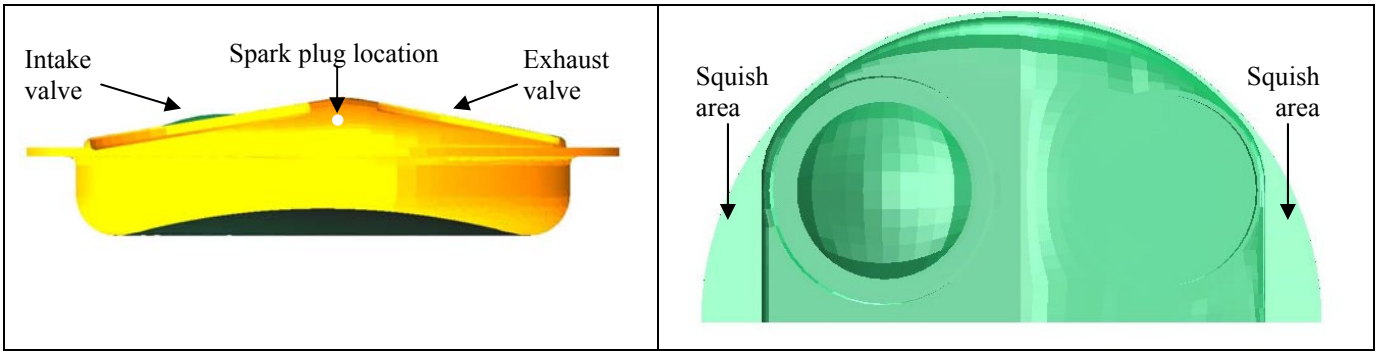

Figure 1 – Drawing of the combustion chamber (left: cross section; right: top view)

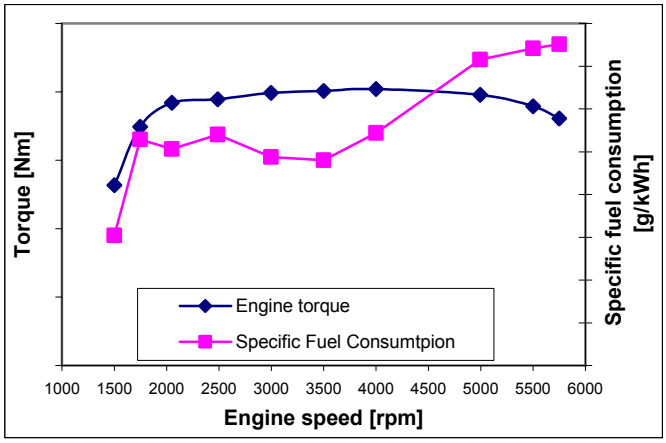

Figure 2 – Measured Engine Performance

Above 2000 rpm, the engine performs very high torque levels, considering its size. It can be noticed that engine torque is almost constant in a wide speed range. The high brake specific fuel consumption highlights the difficulties in turbocharging spark-ignition engines with good efficiencies.

At full load, even if rich mixtures are used, Figure 3 shows that below 2500 rpm it is necessary to retard the spark timing with respect to the top dead center (0 crank angle degree, in the figure) in order to avoid knock.

At high speed, full load operating points, very rich mixtures are used to reduce the exhaust gas temperature in order to protect the engine catalyst [16, 17].

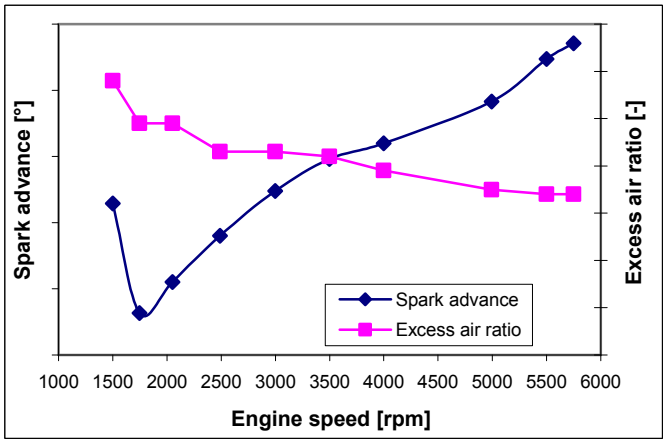

Figure 3 – Engine spark timing and excess air ratio

The first prototype realization highlighted serious detonation risks which could lead to adopt measures lowering the engine thermal efficiency. For this reason, the CFD analysis has been utilized in order to deeply investigate the origins of the knock problem.

NUMERICAL APPROACH

The AVL FIRE 7.3 code has been used to solve the ensemble-averaged governing equations of the flow within the computational domain [18, 19, 20].

The problem of the unknown turbulence correlation is resolved through a compressible version of the standard two equations k-ε model. The partial differential transport equations are discretized on the basis of a finite volume method. The temporal discretization is Euler implicit. Hybrid and Central Total Variation Diminishing differencing schemes are used for the approximation of the spatial derivatives. The coupled set of algebraic equations is solved iteratively based on a pressure-velocity coupling procedure (Semi-Implicit Method for Pressure-Linked Equations algorithm).

Combustion modeling

The complex oxidation process of gasoline fuel during the turbulent combustion process is modeled by a single step irreversible reaction (equation 1):

$$\text{Fuel} + \text{air}(O_2, N_2) \rightarrow \text{products}\ (CO_2, H_2O, N_2) \qquad (1)$$

The mean reaction rate of equation 1 has been evaluated by the coherent flame model. Based on the laminar flamelet concept, the CFM model [21, 22, 23] assumes the mass burning rate per volume unit is proportional to the laminar flame speed (S_L, in equation 2). The proportionality factor is represented by the flame surface density (Σ), determined via a balance equation (equation 3). In this way, the CFM separates the treatment of the chemical problem, reassumed by the overall variable S_L, and the turbulent interactions described by Σ.

$$\dot{w} = \rho_u S_L \Sigma \qquad (2)$$

$$\frac{\partial \Sigma}{\partial t} + \frac{\partial}{\partial x_i}(U_i \Sigma) = \frac{\partial}{\partial x_i}\left(\frac{\nu_t}{\sigma_\Sigma}\frac{\partial \Sigma}{\partial x_i}\right) + S - D \qquad (3)$$

In equation (3), S is the production of flame surface by turbulent rate of strain, while D is the annihilation term due to mutual collisions. The D term is proportional to Σ^2; S term is proportional to the product of the average rate of strain and the flame surface density Σ via an empirical coefficient C. According to the ITNFS model [24, 25] the average rate of strain is considered inversely proportional to the turbulent mixing time, corrected by a function which accounts for the size of turbulence scales and for viscous and transient effects. The laminar flame speed is supposed depending on the fresh gas conditions: the experimental correlations of Metghalchi and Keck are used [26].

Knock modeling

In order to take in account the development of knock at different locations and times in the combustion chamber, an auto-ignition mechanism is considered.

It is impossible, indeed, to simulate the onset of knock using a simple one-step combustion reaction, without considering the chemistry of the pre-reactions occurring in the engine end gas.

The knock model used in this paper, based upon the well known SHELL model, consists of a degenerate-branched-chain mechanism containing: initiation (with radicals production), propagation (whit heat release production) and branching agent formation, branching and two termination steps (linear and quadratic). Species that play a similar role in the ignition chemistry are combined and treated as a single unit; in particular the model considers the hydrocarbon radical (R), the branching agent (B) and the autocatalytic product (Q). The heat release rate per volume unit depends on the radical concentrations [R], while the propagation step rates are calculated by Arrhenius or composed forms. [18, 27].

Grids

The combustion chamber of the engine studied in this paper is symmetric and this allows a 180° grid generation. The combustion chamber, the intake port and the intake manifold have been discretized. Unstructured grids have been generated using hexahedral elements according to the procedure described in [28]. The dynamic grids shown in Figure 4 have about 50.000 cells as a minimum and about 100.000 cells as a maximum.

Initial and boundary conditions

Simulations start at the intake valve opening and finish at the exhaust valve opening. In order to avoid extremely thin cells between the valve and the seat, the intake valve is considered closed for a valve lift smaller than 0.2 mm.

Unsteady gas dynamic calculations, reproducing the engine behavior, have been used to define boundary and initial conditions. Modeling has been performed by means of the well known 1-D, GT-Power code. Calculated and measured volumetric efficiencies at full load and at different speeds have shown a satisfactory agreement.

At inflow boundary the total constant pressure and the temperature are set according to the results obtained by 1-D calculations; as usual in port fuelled injected engine the incoming charge is considered premixed. The integral length scale is assumed equal to 10% of the hydraulic diameter, while the inlet turbulent kinetic energy is set equal to the square of 10% of the inlet mean velocity provided by the 1-D model.

The boundary conditions at solid walls are the no-slip velocity and the constant temperature conditions.

Finally, the homogeneous charge within the cylinder has been considered initially quiescent.

RESULTS

As usual, the model has been validated by comparing the calculated high pressure curves to the measured data provided by the engine manufacturer. Since the experimental activity has been carried out by other researchers, out of the authors' laboratory, a few percentage points discrepancy in the initial and boundary imposed at the computations and those used in the measures is possible.

The CFM has been tuned setting the production constant equal to 1.35 and the destruction constant equal to 1.0. An initial value of the flame surface density equal to 500 1/m in a spherical kernel (r = 4 mm) has been considered to simulate the ignition phase.

In Figure 5, the pressure development for three different engine speeds at full load is reported.

As it can be observed, the behavior at high speeds is quite satisfying, while slight differences rise at 2000 rpm. Probably, this is due to the mentioned initial difference which is more important when charge mass flow rates are small. All in all, the calculated pressure values result in good agreement with the measured data.

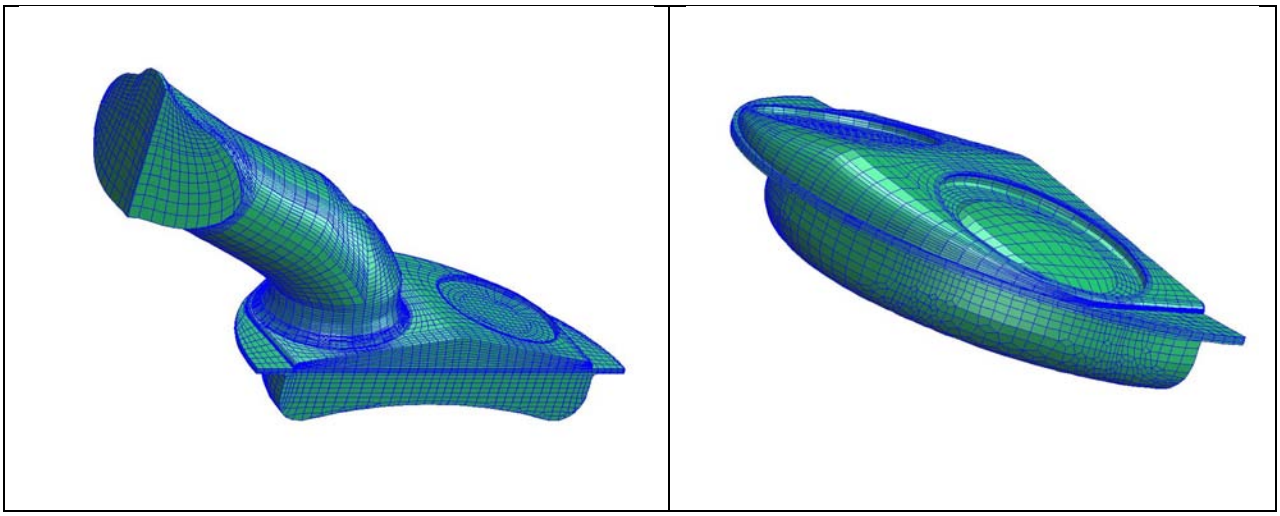

Figure 4 – Engine grids at top dead centers

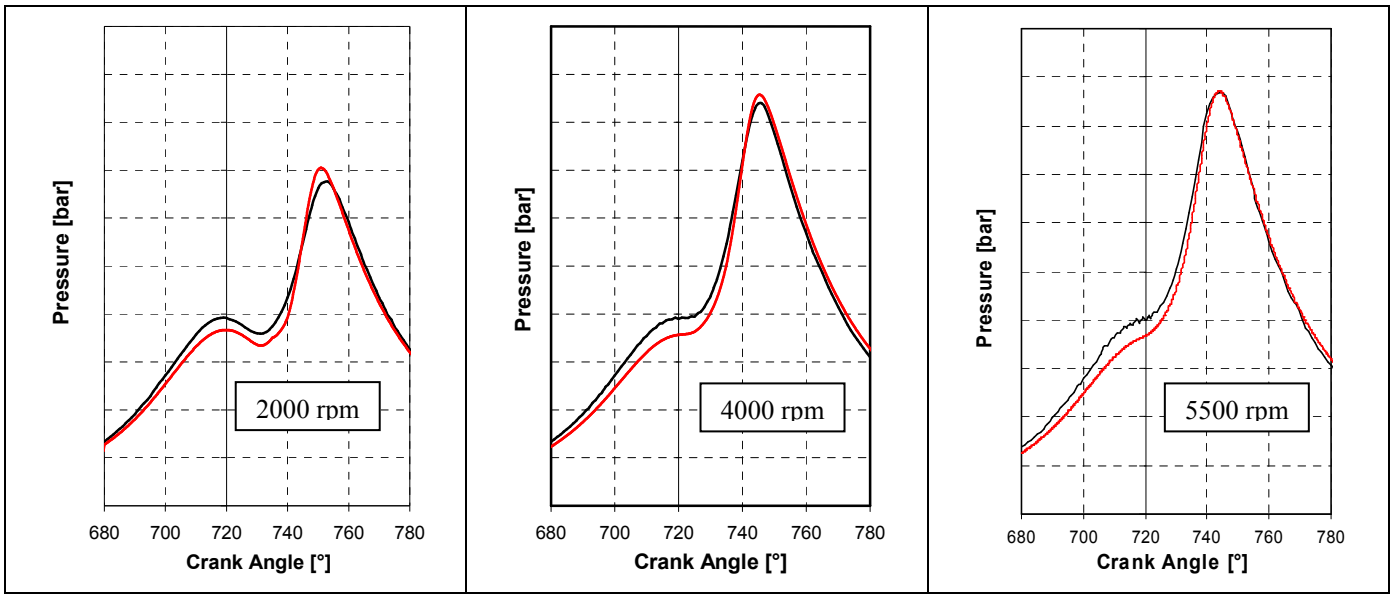

Figure 5 – Comparison of calculated and measured cylinder pressures. Full load (red lines: calculated data; black lines: measured data)

Considering that the worst point presents about a 8% error, the results, at this first step, seem to be satisfying. This encouraged the authors in using the proposed model in order to deeply investigate the behavior of the turbocharged engine.

One of the first problems coming out in development of a spark-ignition turbocharged engine is linked to the flame front propagation and detonation risks. Of course, the increased pressure and temperature levels, with respect to naturally aspirated engines, increase knock risks. When supercharging is used as a means for engine downsizing, thus for achieving higher engine overall efficiency rather than higher performances, a crucial point is to find the proper measures to avoid knock risks without excessively penalizing the engine thermal efficiency, so vanishing the downsizing benefits.

A detailed knowledge of the flow field within the cylinder and propagating characteristics of the flame front is very helpful in suggesting a strategy for increasing the combustion rate and improving the engine knock resistance. To this aim, first the in-cylinder charge motion has been studied.

The four-valve per cylinder engine is characterized by a fairly good mean tumble level. The trend of tumble motion at the operating points 1750 and 5500 rpm, full load is reported in Figures 6 and 7.

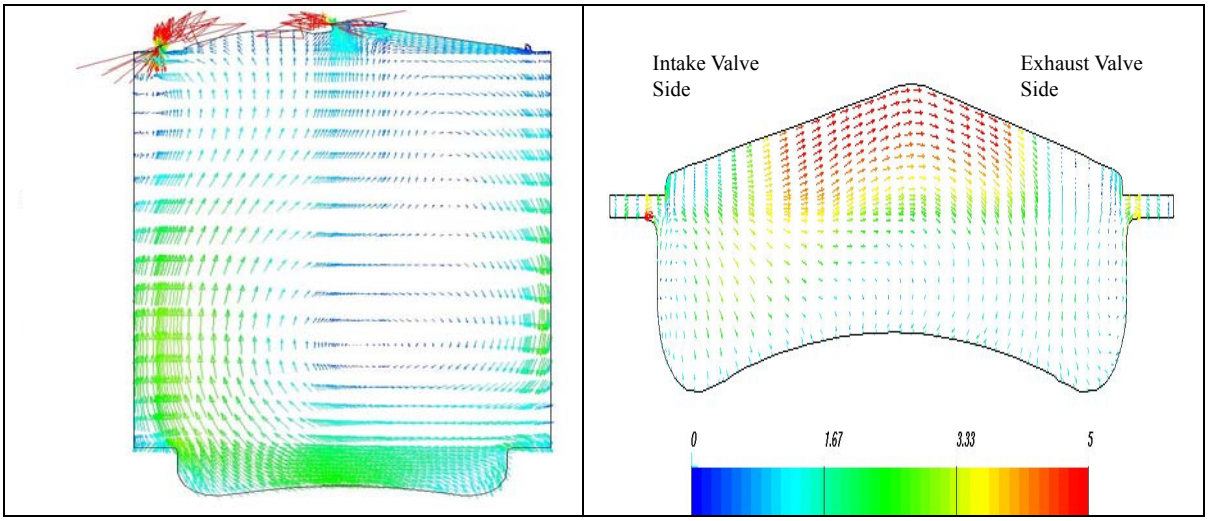

Figure 6a – Tumble motion at IVC, 1750 rpm

Figure 6b – Tumble motion at the spark time, 1750 rpm

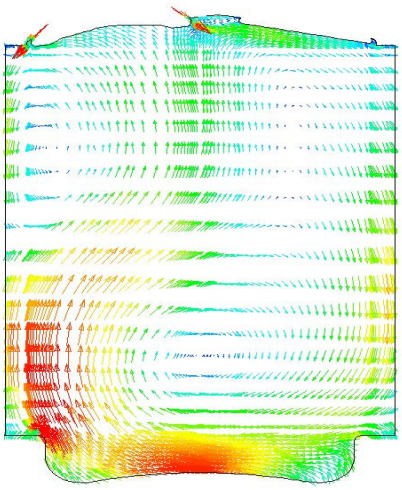

Figure 7a – Tumble motion at IVC, 5500 rpm

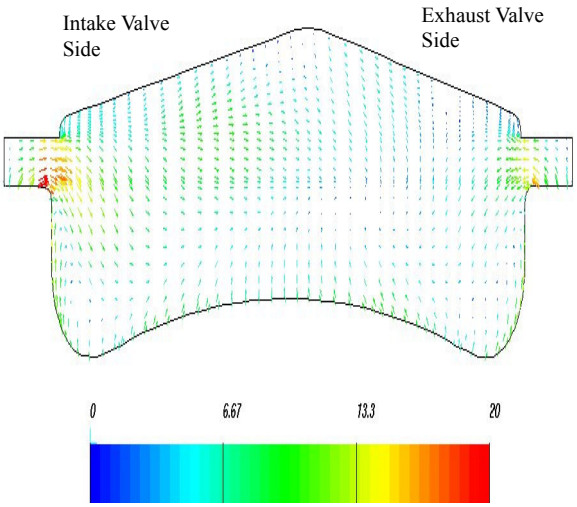

Figure 7b – Tumble motion at the spark time, 5500 rpm

Figures marked a) report the structures of tumble motion at the inlet valve close, while Figures marked b) show tumble at the ignition time. The main difference between these two operating points is visible in eddy structures at the end of suction stroke. At low speed, almost all the entering flow is addressed toward the exhaust valve side of the cylinder and a single large eddy is formed. At higher speed, besides the main eddy growing in the exhaust valve side, the small portion of charge, flowing directly to the cylinder wall beneath the inlet valves, has sufficient kinetic energy to form a second counter-rotating vortex in the top-left corner of the cylinder.

This behavior can explain the values of the average tumble indices calculated at different engine speeds, reported in Figure 8.

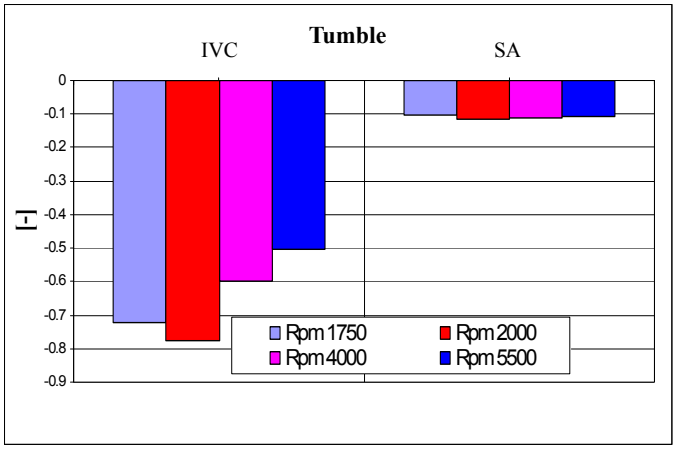

Figure 8 – Mean tumble indices at the inlet valve close (IVC) and at spark timing (SA). Full load, different engine speeds

The tumble ratio has been defined as follows:

$$R_T = \frac{\Gamma_T}{I_T \cdot 2 \cdot \pi \cdot n_s} \qquad (4)$$

where Γ_T and I_T are respectively the charge momentum and moment of inertia, while n_s is the engine speed in revolutions per second.

The formation of the second eddy at speed higher than 2000 rpm, despite the increase in speed and vortex intensity, leads to a decrease, in the mean tumble index at suction end, of more than 30% at 5500 rpm.

In authors' opinion, the most significant result is represented by the direction of velocity vectors at the spark time rather than their intensity. As it can be observed both in Figures 6b and 7b, at the ignition start, the flow field moves the flame towards the exhaust valve zone, generating an heterc SA flame development. Starting from the spark-plug, the flame quickly reaches the cylinder wall beneath the exhaust valves while it takes more time to reach the opposite side. This could be a knock risk area. The flame surface density is reported in Figures 9 and 10 for two engine speeds. The asymmetric flame propagation is clearly visible.

A confirmation of this possibility derives from the observation of the temperature distribution within the combustion chamber as well (Figures 11 and 12).

In this view, the top-right corner of the combustion chamber corresponds to the inlet valve zone. Compared to the opposite side (exhaust valve zone) this portion of the chamber looks colder.

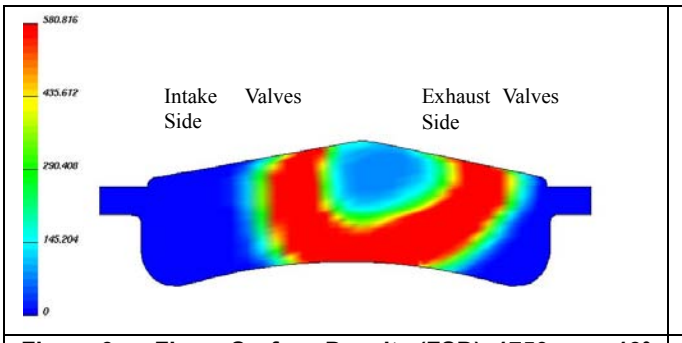

Figure 9a – Flame Surface Density (FSD), 1750 rpm; 13° after ignition

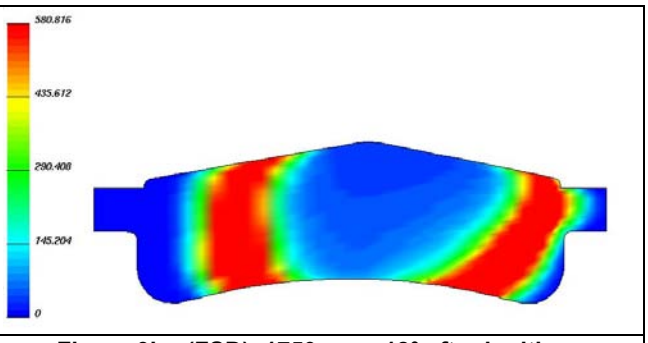

Figure 9b - (FSD), 1750 rpm; 18° after ignition

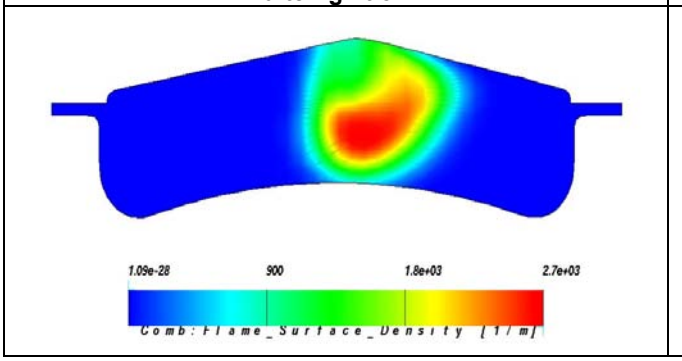

Figure 10a - (FSD), 4000 rpm; 15° after ignition

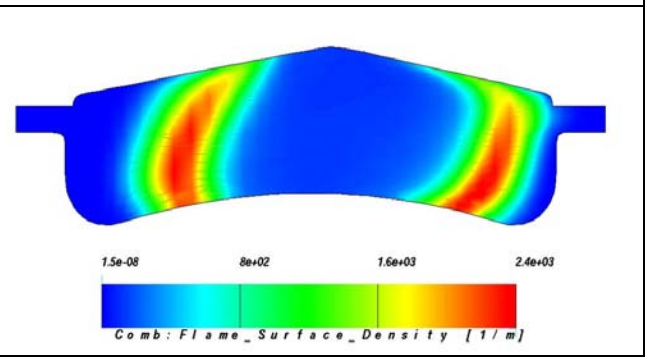

Figure 10b - (FSD), 4000 rpm; 20° after ignition

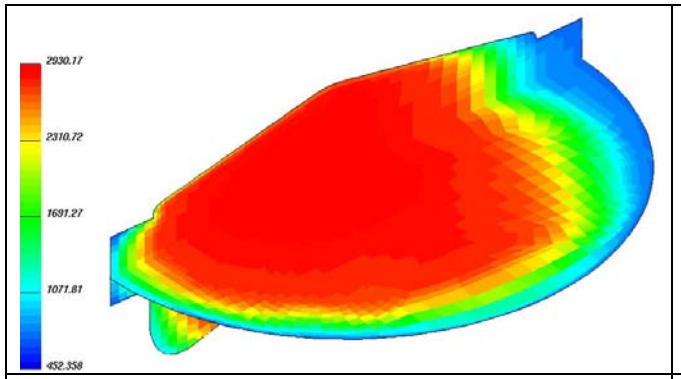

Figure 11a – Temperature distribution. 1750 rpm, 23° after ignition.

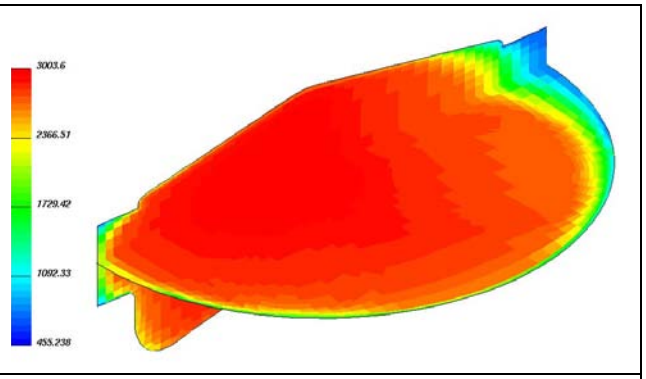

Figure 11b – Temperature distribution. 1750 rpm, 28° after ignition.

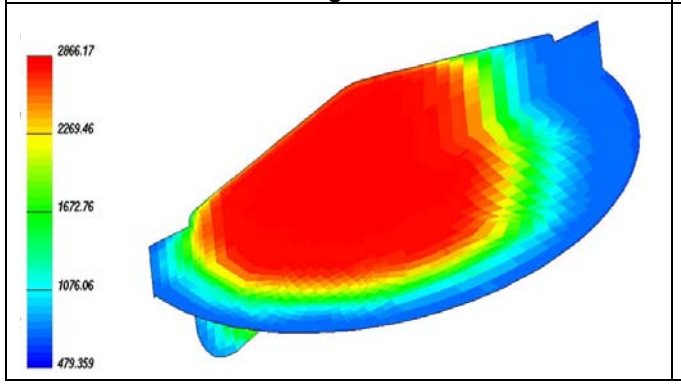

Figure 12a – Temperature distribution. 2000 rpm, 19° after ignition

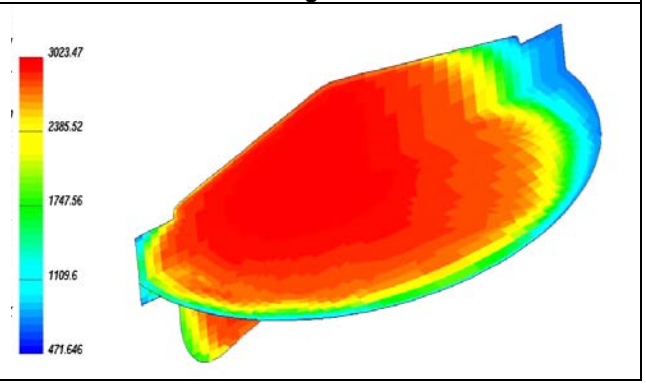

Figure 12b – Temperature distribution. 2000 rpm, 24° after ignition

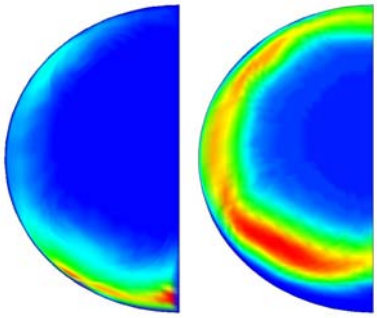

Figure 13a – 1750 rpm; 23° after ignition

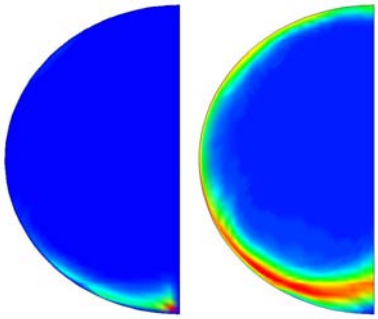

Figure 13b – 1750 rpm; 28° after ignition

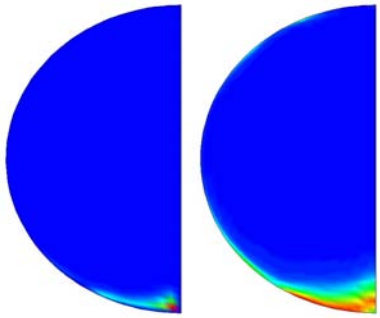

Figure 13c – 1750 rpm; 33° after ignition

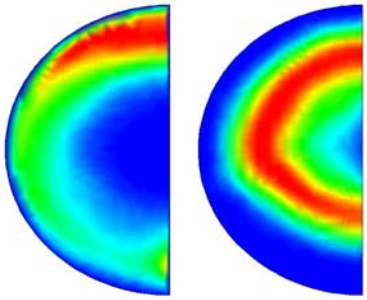

Figure 14a – 2000 rpm; 16° after ignition

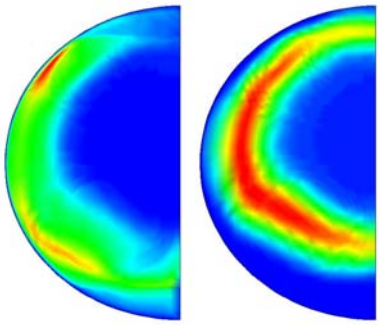

Figure 14b – 2000 rpm; 19° after ignition

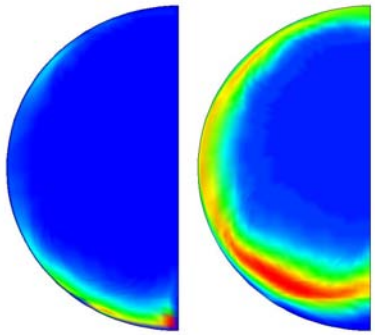

Figure 14c – 2000 rpm; 24° after ignition.

In Figures 13 and 14, in each picture (a,b,c), the calculated detonation risk, according to the Shell model previously described (left), and the flame front propagation (right), for low engine speeds, are reported.

The Shell model seems to confirm previous observations regarding the knock risk. The asymmetric development of the flame front produces a chamber portion reached later by the flame. The end gas in this area could have the necessary time for completing the pre-reaction mechanism and arriving to the auto-ignition.

Even though these results are merely theoretical, it seems reasonable assuming the in-cylinder flow field and the asymmetric development of the flow field as a possible responsible of knock onset.

Modification of engine combustion chamber

In the basis design of the prototype combustion chamber, the flame front, pushed by the charge flow in the volume by the spark plug, moves along a preferential path. Thus, a simple modification of piston geometry has been proposed in order to accelerate and homogenize the flame propagation. The idea is, for a given flow field, to provide a combustion chamber that effectively could be center with respect to the actual core of flame development. Figure 15 shows a cross section of the proposed geometry.

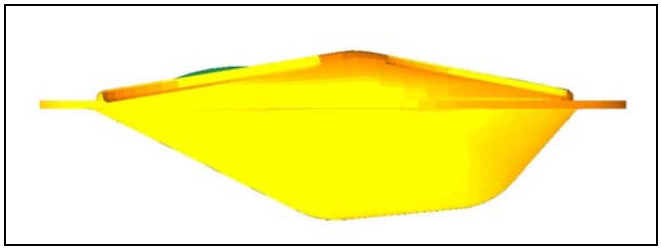

Figure 15 – Combustion chamber cross section of the proposed geometry

Due to the new piston design, the chamber center is translated toward the exhaust valve zone. The engine head and the spark-plug location have not been modified in this analysis and the geometrical compression ratio remained unvaried.

Since the engine knock resistance is the critical point of this discussion, only a low speed (1500 rpm), full load point has been analyzed. Intake, compression, combustion and expansion processes have been simulated again. In the combustion model, the same characteristic constants used for the previous geometry have been kept.

In Figure 16, a comparison of calculated turbulence indices for the two different combustion chambers is reported.

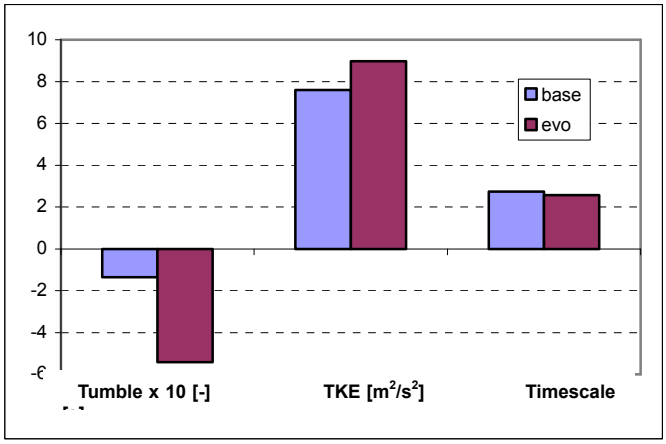

Figure 16 - Tumble indice, mean Turbulent Kinetic Energy and mean Turbulent Mixing Time calculated at TDC for the baseline combustion chamber (base) and for the proposed geometry (evo). 1500 rpm, full load.

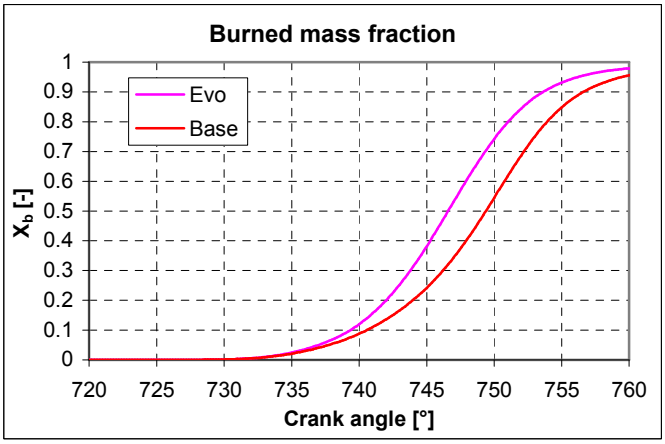

Figure 17 - Comparison of mass fraction burned, for the baseline combustion chamber (base) and for the proposed geometry (evo); same spark advance (spark timing 727°)

The proposed geometry provides higher tumble levels (four times), at the end of compression, and the turbulent kinetic energy features a 25% increase.

In Figure 17, a comparison of mass fractions burned (X_b) is shown.

Images in Figure 18 show a significantly higher flame propagation rate obtained by the proposed geometry (evo). Furthermore, the flame front propagation is visibly more symmetric and the end-gas area is more homogenously distributed at the periphery of the combustion chamber.

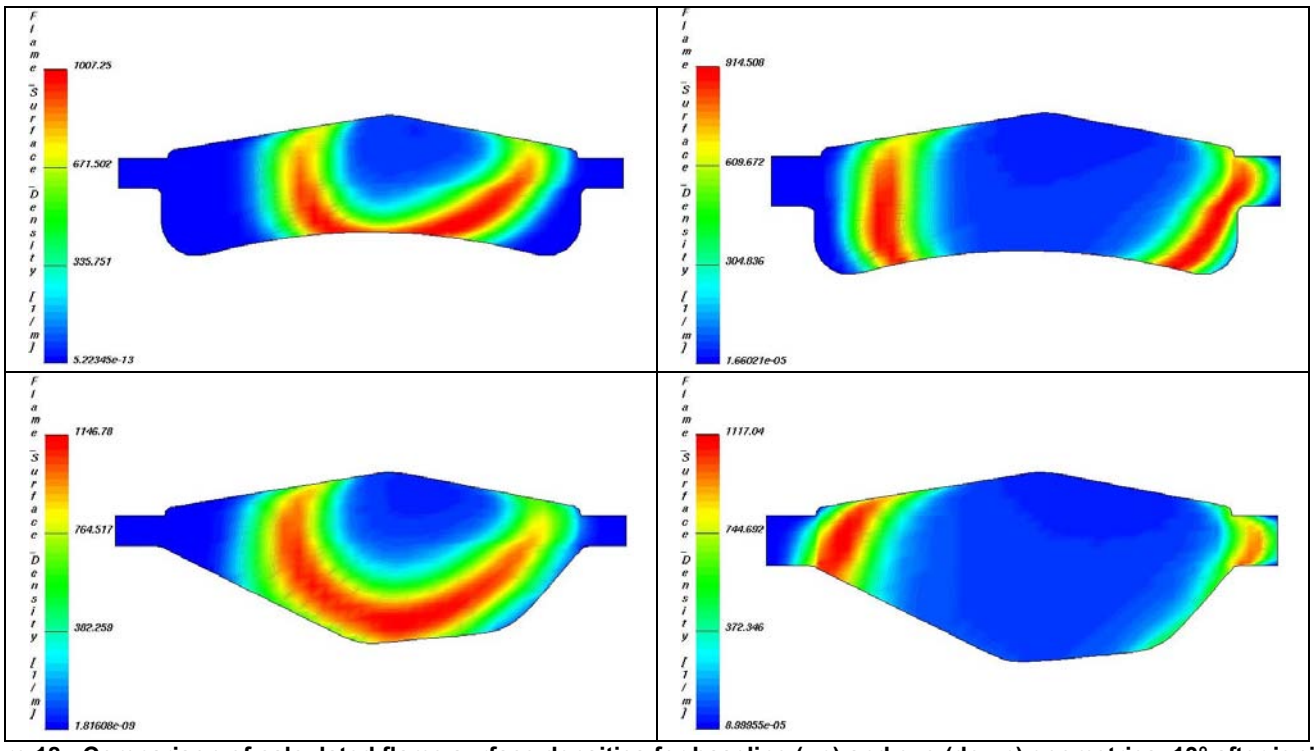

Figure 18 - Comparison of calculated flame surface densities for baseline (up) and evo (down) geometries, 13° after ignition (left) and 20° after ignition (right)

These circumstances let foresee the new proposed geometry, at given conditions, could perform a lower knock risk or allow a better spark timing. Of course, the faster combustion process improves the engine thermal efficiency: considering both the pumping work calculated by the 1-d simulations and the high pressure cycle predicted by the 3-d analysis, it has been estimated that, for the operating point used as an example, 1750 rpm, full load, the specific fuel consumption decreases from 305.6 g/kWh (baseline geometry) to 295 g/kWh (modified combustion chamber).

Timing and location of knock onset depend on both the state of the in-cylinder end gas and the time needed by the flame front to sweep the end gas zone. In particular, the unburned gas temperature governs the pre-reaction rate in the end gas that leads to thermal auto-ignition. The amount of species predicted by the shell model can be assumed as an indicator of the knock onset probability. Of course, it is important to correlate the specie concentrations with the amount of unburned fuel in the end gas thus to obtain information on knock intensity.

In Figures 19 the maximum concentrations of calculated radical R and intermediate Q products versus the calculated mass fraction burned, for different studied cases, are shown.

Considering that for the baseline geometry the engine runs below the knock limit, calculations seem to show that also the results obtained for the new geometry are knock free; small ignition timing improvement could be possible.

It is worth noting that evo geometry shows a knock onset location different from that of the base geometry (see picture 20 as an example). The new bowl makes easy the flame front propagation along the symmetry plane, removing the knock risk in the zone A of the baseline geometry. For the new geometry the critical end gas zone is concentrated below the intake valve, close to the cylinder liner. Maybe, a different piston crown design, able to produce a reverse squish motion during the expansion stroke, could be useful in order to reduce the knock risk [29].

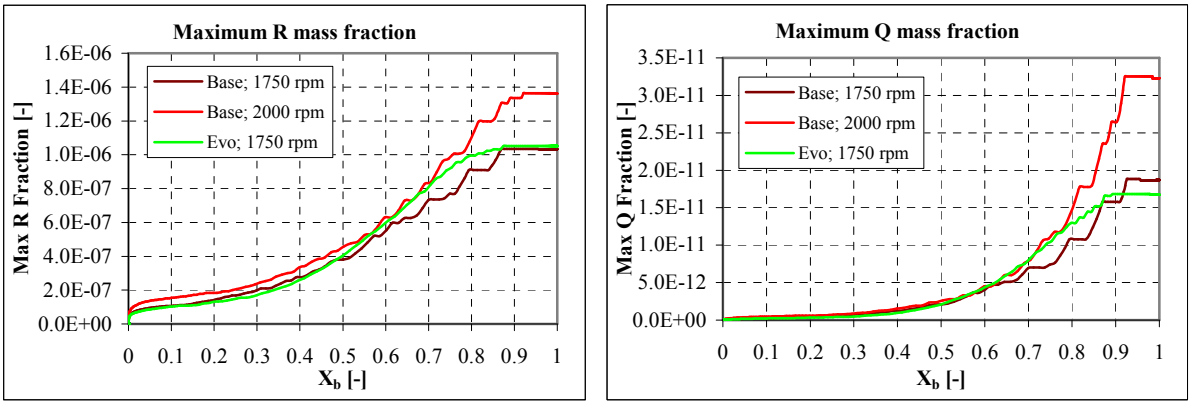

Figure 19 – Maximum value of both radical R and intermediate Q product concentrations calculated in the computational domain versus the calculated overall burnt mass fraction for the cases studied

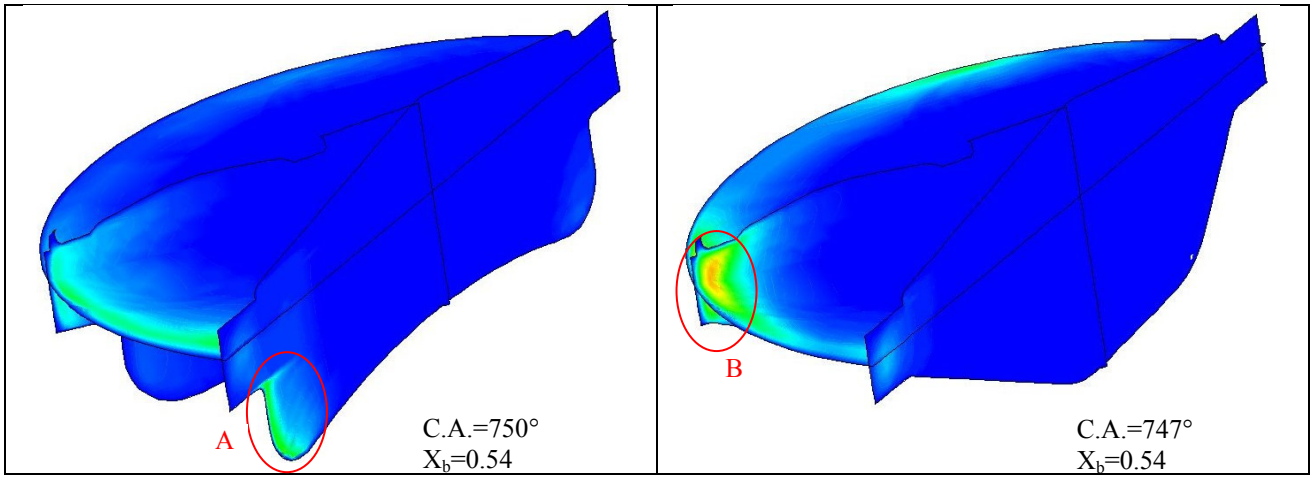

Figure 20 – Comparison of the detonation risk calculated for baseline prototype (left) and evo geometry (right)

CONCLUSION

The behavior of a small turbo-charged spark-ignition engine prototype has been numerically analyzed. In this first study, the major attention has been paid to the combustion development and the problem of knock onset rather than to the estimation of engine performance.

Calculations have performed using AMD 2.8Ghz computer with SUSE Linux operative system; the mean calculation time was about 144 hours for each case.

In order to analyze such aspects as combustion rate and flame front propagation, the flow field within the cylinder has been investigated. The 3-D AVL Fire code has been utilized. The engine geometry has been reproduced constructing the mesh for the intake manifold and port and for the combustion chamber. The model was validate by comparing the calculated pressure curves to the measured data provided by research center of the prototype manufacturer.

Since the first prototype realization showed serious detonation risks, the CFD analysis has been utilized in order to deeply investigate the development of the combustion process.

The obtained results highlighted a fairly good tumble level and, mainly, a particular flow field inducing a preferential path to the charge. This generated an asymmetric development of the flame front and, as a consequence, the rise of a late burning zone. The knock model indicated this area as a knock risk area. In order to improve the combustion development and make the flame front actually centered around the spark plug, a modified piston geometry has been proposed by the authors.

The proposed virtual prototype performed higher combustion rate and improved (symmetric) flame development thus providing higher engine thermal efficiency and lower knock risks.

This paper is a first work dealing with the spark-ignition engine downsizing. In a near future the performance advantages coming from this technique will be widely analyzed. At the end, the paper could represent a further contribution giving evidence to the effectiveness of CFD analysis in both investigating complex phenomena and predicting the performance of virtual prototypes, saving expensive and time consuming experimental tests.

REFERENCES

1. N. Watson and M.S. Janota, “Turbocharging the Internal Combustion Engine”, John Wiley, New York, 1982.
2. R.M. Heavenrich, “Light-Duty Automotive Technology and Fuel Economy Trends Through 1999”, US EPA Report EPA420-R-99-018.
3. P. Leduc, B. Dubar, A. Ranini, and G. Monnier, “Downsizing of Gasoline Engines: an Efficient Way to Reduce CO_2 Emissions”, Oil and Gas Science and technology - Rev. IFP, Vol. 58 (2003), No. 1, pp. 115-127.
4. B. Lecointe and G. Monnier, “Downsizing a Gasoline Engine Using Turbocharging with Direct Injection”, SAE Paper no. 2003-01-0542.
5. J. Stokes, T.H. Lake and R.J. Osborne, “A Gasoline Engine Concept for Improved Fuel Economy – The Lean Boost System”, SAE Paper no. 2000-01-2902.
6. M. Wirth, U. Mayerhofer, W.F. Piock and G.K. Fraidl, “Turbocharging the DI Gasoline Engine”, SAE Paper no. 2000-01-0251.
7. T. Lake, J. Stokes et al., “Turbocharging Concepts for Downsized DI Gasoline Engines”, SAE Paper no. 2004-01-0036.
8. D. Petitjean et al., “Advanced Gasoline Engine Turbocharging Technology for Fuel Economy Improvements”, SAE Paper no. 2004-01-0988.
9. J.I. Ramos, “Internal Combustion Engine Modeling”, Hemisphere, Publ. Corp., 1989.
10. W. K. Cheng and J. A. Diringer, “Numerical Modeling of SI Engine Combustion with a Flame Sheet Model”, SAE Paper 910268, 1991
11. G. Fontana, E. Galloni, R. Palmaccio, “Experimental and numerical analysis of a small VVT-SI engine”, SAE Paper no. SAE-NA 2005-24-079.
12. P. de Alexandria Cruz, J. N. de Souza Vianna and C. de Silva Moreira, “Study of the Turbulence Intensity Variation Within the Combustion Chamber of a SI Engine due to Turbocharging”, SAE Paper no. 2003-01-3687.
13. J. Navrátil, J. Macek, M. Polášek, “Simulation of a small turbocharged gasoline engine in transient operation”, SAE Paper no. 2004-01-0995.
14. R. J. Pierik, J. F. Burkhard, “Design and Development of a Mechanical Variable Valve Actuation System”, SAE Paper no. 2000-01-1221.
15. F. Bozza, A. Gimelli, R. Tuccillo, “The control of a VVA-equipped SI engine operation by means of 1-D simulation and mathematical optimization” SAE Paper no. 2002-01-1107.
16. R. Fiorenza, M. Pirelli, E. Torella et al., “VVT + Port Deactivation Application on a Small Displacement SI 4 Cylinder 16V Engine: an Effective Way to Reduce Vehicle Fuel Consumption”, SAE paper no. 2003-01-0020.
17. P. Pallotti, E. Torella, J. New, M. Criddle and J. Brown, “Application of an Electric Boosting System to a Small, Four Cylinder S.I. Engine”, SAE Paper no. 2003-32-0039.
18. AVL FIRE Handbook, Version 7, April 2000, Internal Report
19. Tatschl R., Wieser K., Reitbauer R., “Multidimensional Simulation of Flow Evolution, Mixture Preparation and Combustion in a 4-Valve SI Engine”, Third International Symposium on

Diagnostic and Modeling of Combustion in Internal Combustion Engines, Yokohama, 1994
20. R. Tatschi and H. Riediger, “PDF Modelling of Stratified Charge SI Engine Combustion”, SAE Paper 981464, 1998
21. Cheng, W. K., and Diringer, J. A., 1991, “Numerical Modeling of SI Engine Combustion with a Flame Sheet Model”, SAE Paper 910268.
22. Poinsot, T. J., Haworth D. C., and Bruneaux, G., 1993, Combustion and Flame, 95.
23. P. Boudier, S. Henriot, T. J. Poinsot and T. Baritaud, 1992, 24th Symposium (International) on Combustion, The Combustion Institute, Pittsburgh, p. 503.
24. C. Meneveau and T. Poinsot, "Stretching and quenching of flamelets in premixed turbulent combustion." Combustion Flame”, 1991
25. C. R., Choi and K. Y. Huh, “Development of a Coherent Flamelet Model for a Spark-Ignited Turbulent Premixed Flame in a Closed Vessel”, Combustion and Flame, 1998.
26. M. Metghalchi and J.C. Keck, "Burning velocities of mixtures of air with methanol, isooctane and indolene at high pressure and temperature.″ Combustion and Flame” 1982
27. M.P. Halstead, L.J. Kirsch, A. Prothero and C.P. Quinn: ”A Mathematical Model for Hydrocarbon Autoignition at High Pressures”, Proc. R. Soc. Lond. A., 364, pp.515-538, 1975
28. G. Fontana, E. Galloni and R. Palmaccio, “Development of a New Intake System for a Small Spark-Ignition Engine: Modeling the Flow through the Inlet Valve”, SAE Paper no. 2003-01-0369, 2003.
29. T. Ueda, T. Okumura, S. Sugiura and S. Kojima, “Effects of Squish Area Shape on Knocking in a Four-Valve Spark Ignition Engine”, SAE Paper no. 1999-01-1494, 1999